Phase transitions in dense hydrogen - helium plasmas

Vladimir Filinov*, Pavel Levashov*, Michael Bonitz† and Vladimir Fortov*

*Institute for High Energy Densities, Izhorskaya 13/19, 125412 Moscow, Russia
†Christian-Albrechts-Universität zu Kiel, Institut für Theoretische Physik und Astrophysik, Leibnizstr. 15, 24098 Kiel, Germany

Abstract. In this paper we study thermodynamic properties of hydrogen-helium mixtures with the help of direct Path-Integral Monte Carlo simulations. Presented are preliminary results of pressure and energy isotherms in the range from 10^4 K to $2 \cdot 10^5$ K in comparison with available theoretical and experimental results. In the density region, where experiments have observed a sharp conductivity rise the simulations yield indicator for one or two plasma phase transitions, in accordance with earlier predictions.

INTRODUCTION

Many astrophysical problems require the knowledge of thermodynamic properties of hydrogen and helium [1–5]. To understand different effects in stellar structure and evolution one should provide accurate modelling of the underlying physics including equation of state (EOS) effects. In normal stars where there plasma is fully-ionized and almost ideal the construction of EOS doesn't reveal particular difficulties. However the investigation of the giant planets Jupiter and Saturn, and to a lesser extent brown dwarfs demands thermodynamic information for hydrogen and helium in the approximate range of temperatures 1000 K $< T <$ 100000 K and mass densities $0.01 < \rho < 100$ g/cm^3. In this region the complexity of an EOS calculation increases considerably when nonideal effects are compounded with chemical reactions associated with partial pressure dissociation and ionization equilibria [6–10]. Moreover, in this region the the so-called plasma phase transition (PPT) has been predicted [9, 10]. Significant efforts have been made in the last decades to understand the behaviour of dense fully-ionized and partially-ionized hydrogen and helium (see, for example, [8] and references therein). In these works mostly the chemical picture is applied for the calculation of thermodynamic properties. The chemical picture assumes that bound configurations, such as atoms and molecules, retain a definite identity and interact through pair potentials; in other words, this model is valid only at weak interparticle interactions. However at densities corresponding to pressure ionization the electrons in bound configurations become delocalized and bound species lose their identity [11]. Therefore there is a great interest in direct first-principle numerical simulations of strongly coupled degenerate systems which avoid such approximations.

In this work we use the direct path integral Monte Carlo (DPIMC) method to calculate the thermodynamic properties of hydrogen - helium mixtures. This method is well

established theoretically and allows the treatment of quantum and exchange effects without any preliminary physical approximations. Using the results of our simulations we analyze the problem of plasma phase transition in dense hydrogen - helium mixtures.

DIRECT PATH INTEGRAL MONTE CARLO

Path integral Monte Carlo [12, 13] is based upon Feynman's formulation of quantum-statistical mechanics using path integrals [14]. In this work we consider hydrogen - helium mixtures at temperatures from 10^4 K to $2\cdot 10^5$ K and electron particle densities from 10^{20} to $3\cdot 10^{24}$ cm^{-3}. Under such conditions electrons are degenerate while protons and α-particles can be treated as classical particles because of their relatively large masses. Thus for the case of electro-neutral hydrogen-helium plasma with volume V the partition function Z is given by

$$Z(N_e,N_p,N_\alpha,V,\beta)=\frac{1}{N_e!N_p!N_\alpha!}\sum_\sigma\int_V dq_p dq_\alpha\, dr\,\rho(q_p,q_\alpha,r,\sigma;\beta). \qquad (1)$$

Here N_e, N_p, and N_α are the number of electrons, protons, and α-particles, $\beta=1/k_BT$, T is the temperature, $q_p\equiv\{\mathbf{q}_{p1},\mathbf{q}_{p2},\cdots,\mathbf{q}_{pN_p}\}$, $q_\alpha\equiv\{\mathbf{q}_{\alpha1},\mathbf{q}_{\alpha2},\cdots,\mathbf{q}_{\alpha N_\alpha}\}$ are coordinates of protons and α-particles, respectively, $r\equiv\{\mathbf{r}_1,\mathbf{r}_2,\cdots,\mathbf{r}_{N_e}\}$ are the coordinates of electrons, and $\sigma\equiv\{\sigma_1,\sigma_2,\cdots,\sigma_{N_e}\}$ are the spin variables of the electrons. The density matrix in (1) is expressed via a path integral:

$$\int_V dR^{(0)}\sum_\sigma\rho(R^{(0)},\sigma;\beta)=\sum_P\sum_\sigma(-1)^{\kappa_P}\int_V dR^{(0)}\cdots dR^{(n)}\times$$
$$\rho^{(1)}\rho^{(2)}\cdots\rho^{(n)}S(\sigma,\hat{P}\sigma')\hat{P})\rho^{(n+1)}, \qquad (2)$$

where $\rho^{(i)}=\rho(R^{(i-1)},R^{(i)};\Delta\beta)\equiv\left\langle R^{(i-1)}\left|e^{-\Delta\beta\hat{H}}\right|R^{(i)}\right\rangle$, $\Delta\beta\equiv\beta/(n+1)$, $\hat{P}$ is the permutation operator, κ_P is the parity of permutation, S is the spin matrix, $\hat{H}$ is Hamiltonian of the system, $\hat{H}=\hat{K}+\hat{U}_C$, $\hat{K}$ is the kinetic energy, $\hat{U}_C$ is the potential energy, consisting of Coulomb interaction of electrons (e), protons (p), and α-particles (α): $\hat{U}_C=\hat{U}_C^p+\hat{U}_C^e+\hat{U}_C^\alpha+\hat{U}_C^{ep}+\hat{U}_C^{e\alpha}+\hat{U}_C^{p\alpha}$. We denote particle coordinates as follows: $R^{(i)}=(q_p,q_\alpha,r_i)$, $i=1,\cdots,n+1$, $R^{(0)}\equiv(q_p,q_\alpha,r)$, $R^{(n+1)}\equiv R^{(0)}$, $\sigma'=\sigma$. Thus electrons participating in the simulation are represented as fermionic loops with n vertexes: $[R]\equiv[R^{(0)};R^{(1)};\cdots;R^{(n)};R^{(n+1)}]$. Exchange effects for Fermi statistics are taken into account by the permutation operator $\hat{P}$ and the sum over the permutations with parity κ_P. It is possible to reduce the expression (2) to a form in which the sum over all permutations is replaced by the determinant of the exchange matrix $\psi_{ab}^{n,1}$. This technique allows us to improve the accuracy of simulation for strongly degenerate plasma:

$$\sum_\sigma\rho(q_p,q_\alpha,r,\sigma;\beta)=\frac{1}{\lambda_p^{3N_p}\lambda_\alpha^{3N_\alpha}\lambda_\Delta^{3N_e}}\sum_{s=0}^{N_e}\rho_s([R],\beta),$$

$$\rho_s([R],\beta) = \frac{C^s_{N_e}}{2^{N_e}} \exp\{-\beta U([R],\beta)\} \prod_{l=1}^{n} \prod_{m=1}^{N_e} \phi^l_{mm} \det \left| \psi^{n,1}_{ab} \right|_s . \qquad (3)$$

Here $\lambda_p^2 = 2\pi\hbar^2\beta/m_p$, $\lambda_\alpha^2 = 2\pi\hbar^2\beta/m_\alpha$, $\lambda_\Delta^2 = 2\pi\hbar^2\Delta\beta/m_e$, m_p, m_α, m_e are the masses of proton, α-particle and electron, respectively. In equation (3) $U = U^{pp} + U^{\alpha\alpha} + U^{p\alpha} + \sum_{l=1}^{n}\{U_l^{ee} + U_l^{ep} + U_l^{e\alpha}\}/(n+1)$ and $\phi^l_{mm} \equiv \exp\left[-\pi \left|\xi_m^{(l)}\right|^2\right]$ are functions generated from the kinetic energy density matrix, $\xi^{(1)}, \cdots, \xi^{(n)}$ are dimensionless distances between neighbor vertexes of fermionic loops which represent electrons $[R] \equiv [R^{(0)}; R^{(0)} + \lambda_\Delta \xi^{(1)} + \lambda_\Delta(\xi^{(1)} + \xi^{(2)}; \cdots]$. Elements of the exchange matrix $\psi^{n,1}_{ab}$ are defined by the expression:

$$\left\| \psi^{n,1}_{ab} \right\|_s \equiv \left\| \exp\left\{ -\frac{\pi}{\lambda_\Delta^2} |(r_a - r_b) + y_a^n|^2 \right\} \right\|, \; y_a^n = \lambda_\Delta \sum_{k=1}^{n} \xi_n^{(k)}.$$

The index s stands for the number of electrons with same spin projection.

As a high-temperature density matrix one can use its asymptote in the limit $T \to \infty$. Every N-particle high-temperature density matrix can be represented as a product of two-particle density matrices. For the two-particle density matrix there is an analytical solution of the Bloch equation by first-order perturbation theory [16]:

$$\rho(\mathbf{r}_a, \mathbf{r}'_a, \mathbf{r}_b, \mathbf{r}'_b, \beta) = \frac{m_a m_b}{(2\pi\hbar^2\beta)^3} \exp\left[-\frac{m_a}{2\hbar^2\beta}(\mathbf{r}_a - \mathbf{r}'_a)^2\right] \exp\left[-\frac{m_b}{2\hbar^2\beta}(\mathbf{r}_b - \mathbf{r}'_b)^2\right] \exp\left[-\beta\Phi^{ab}\right],$$

where $\Phi^{ab}(\mathbf{r}_a, \mathbf{r}'_a, \mathbf{r}_b, \mathbf{r}'_b, \beta)$ — nondiagonal effective two-particle pseudopotential:

$$\Phi^{ab}(\mathbf{r}_a b, \mathbf{r}'_a b, \beta) = e_a e_b \int_0^1 \frac{d\alpha}{d_{ab}(\alpha)} \mathrm{erf}\left(\frac{d_{ab}(\alpha}{2\lambda_{ab}\sqrt{\alpha(1-\alpha)}}\right). \qquad (4)$$

Here $d_{ab}(\alpha) = |\alpha\mathbf{r}_{ab} + (1-\alpha)\mathbf{r}'_{ab}|$, $0 \le \alpha \le 1$, $\mathrm{erf}(x) = 2/\sqrt{\pi}\int_0^x \exp(-t^2)\,dt$ denotes the error function, $\lambda_{ab}^2 = \hbar^2\beta/2\mu_{ab}$, e_a, e_b are the charges of particles, m_a, m_b are the masses of particles, $\mu_{ab}^{-1} = m_a^{-1} + m_b^{-1}$ are reduced mass. In the limit of high temperature two-particle nondiagonal effective potential can be approximated by a half-sum of diagonal pseudopotentials (4):

$$\Phi^{ab}(|\mathbf{r}_{ab}|, \Delta\beta) = \frac{e_a e_b}{\lambda_{ab} x_{ab}} \left\{1 - \exp(-x_{ab}^2) + \sqrt{\pi} x_{ab}[1 - \mathrm{erf}(x_{ab}]\right\}, \qquad (5)$$

where $x_{ab} = |\mathbf{r}_{ab}|/\lambda_{ab}$. It is worth to underline that $\Phi^{ab}(|\mathbf{r}_{ab}|, \Delta\beta)$ tends to a finite value at $x_{ab} \to 0$ and to the Coulomb potential $e_a e_b / x_{ab}$ at $x_{ab} \to \infty$. It is proved that the pseudopotential (5) coincides with an exact quantum potential at temperatures $T > 2 \cdot 10^5$ K [17]. U^{ln} and U_l^{ln} in Eq. (3) is the sum of the effective quantum pair interaction between two charged plasma particles described by the Φ^{ab}.

All thermodynamic properties can be expressed through the partition function derivatives. For example, pressure and total energy are given by the formulas:

$$E = -\beta \partial \ln Z / \partial \beta,$$
$$\beta P = \partial \ln Q / \partial V = [\eta / 3V \partial \ln Q / \partial \eta]_{\eta=1} \quad . \tag{6}$$

Multiple integrals in the formulas (6) are calculated with the help of the standard Metropolis technique in a cubic cell with periodic boundary conditions [12]. The accuracy ε of the calculations depends on the number of factors n in the equation (2), temperature T and electron degeneracy parameter $\chi = n_e \lambda_e^3$ and is given by expression – $\varepsilon \sim (\beta \mathrm{Ry})^2 \chi / (n+1)$, where n_e is the particle density of electrons, $\lambda_e^2 = 2\pi\hbar^2\beta/m_e$ [18]. According to this estimation to simulate a Coulomb system at the temperature 10^4 K it is sufficient to choose $n = 20$. High temperature density matrix in Eq. (2) relates in this case to temperature higher than Ry.

SIMULATION RESULTS

We tested our computational scheme by many ways. First of all we calculated thermodynamic properties of ideal hydrogen plasma [19] and found very good agreement up to degeneracy parameter $\chi = 10$. To extend the region of degeneracy parameter we improved the treatment of exchange effects. Unlike the previous version of the method [12] in this work we take into account exchange effects not only inside the main Monte Carlo cell but also with the neighboring periodic images. It is necessary to include such procedure into the algorithm if the electron thermal wavelength is comparable or larger than the size of the Monte Carlo cell. Thus the exchange interaction was calculated in the nearest 3^3, 5^3 etc. Monte Carlo cells in accordance with the value of electron thermal wavelength. The accuracy of exchange effects treatment was controlled by comparing the results of calculations with analytical dependences for pressure and energy of ideal degenerate plasma.

We also studied interacting hydrogen plasma in a wide range of temperatures and particle densities [20, 21]. The DPIMC method allowed us to investigate the effects of temperature and pressure dissociation and ionization *ab initio*. From the analysis of pair distribution functions we observed the formation and break-up of molecules and atoms under different conditions. At very high density we also observed the effect of proton ordering indicating the formation of Coulomb crystal. We found rather good agreement with the calculations performed by other methods at small and medium densities. However at high values of plasma density in the region of pressure ionization no reliable analytical methods exist.

The simulation results for hydrogen plasma in the region of temperatures from $T = 10^4$ K to 10^6 K and electron particle densities from $n_e = 10^{22}$ cm^{-3} to 10^{24} cm^{-3} allowed us to calculate the deuterium shock Hugoniot [22]. It is interesting to note that the resulting curve is located between the experimental data of Knudson *et al.* [23] and Collins *et al.* [24].

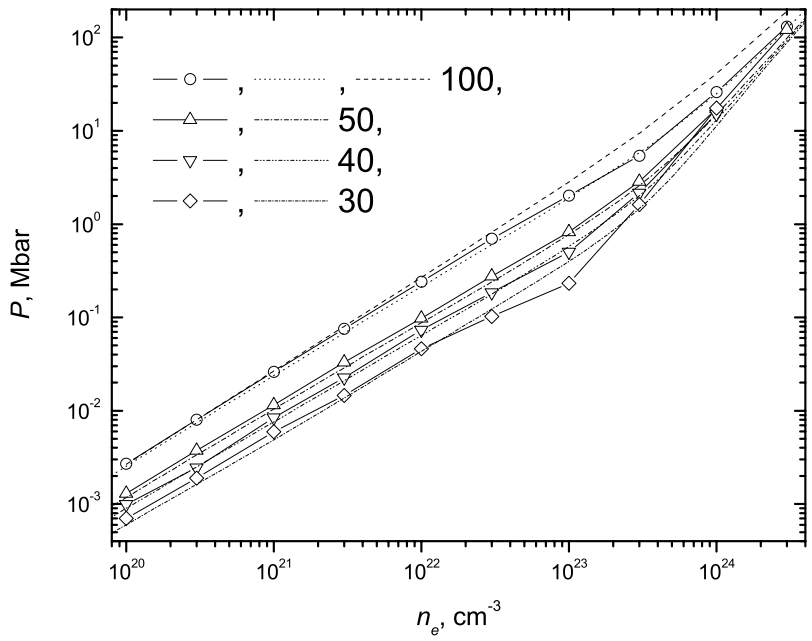

FIGURE 1. Pressure in a hydrogen-helium mixture with the mass concentration of helium $Y = 0.234$. Shown are isotherms calculated with the help of DPIMC method (lines with symbols) and related isotherms from [2, 7] (lines without symbols). Shown on the picture numbers are temperatures in units of thousand Kelvin. For $T = 100000$ K the dashed line presents the EOS for ideal plasma.

In this work we apply our computational scheme to the thermodynamic properties simulations of hydrogen-helium mixture with a composition corresponding to that of the outer layers of the Jovian atmosphere. During the mission of the Galileo spacecraft the helium abundance in the atmosphere of Jupiter was determined as $Y = m_{He}/(m_{He} + m_H) = 0.234$ and was close to the present-day protosolar value $Y = 0.275$. As the model of the Jupiter is significantly determined by its composition and EOS it is interesting to simulate the thermodynamic properties of the mixture with such composition in the region of pressure dissociation and ionization where traditional chemical models of plasma fail.

We carried out the calculations of thermodynamic properties of hydrogen - helium mixture in the region of temperatures from $T = 10^4$ K to $2 \cdot 10^5$ K and electron densities from $n_e = 10^{20}$ cm^{-3} to $3 \cdot 10^{25}$ cm^{-3}. First of all we compare our results with available data on hydrogen-helium mixture of [2, 7]. This model is based on the chemical picture with classical statistics for molecules and ions and Fermi-Dirac statistics for the electrons. It takes into account a lot of physical effects including dissociation and ionization, interactions between charged particles and neutral atoms and molecules, neutral-neutral interactions, high-pressure screening effects, excited electronic states of molecules as well as a number of "second-order" phenomena. Owing to the complexity of of the

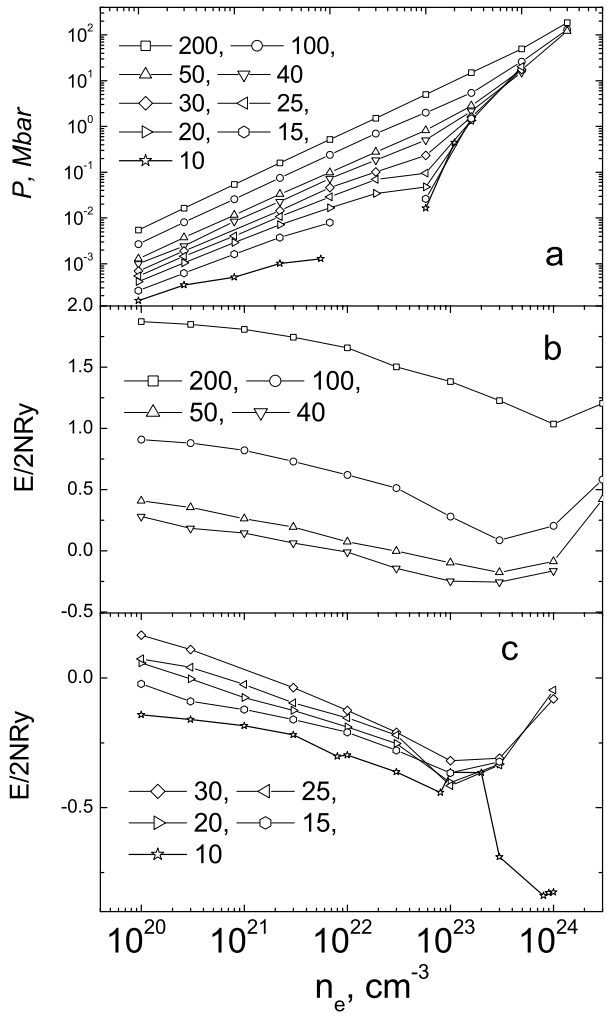

FIGURE 2. Pressure a) and energy b,c) in a hydrogen-helium mixture with the mass concentration of helium $Y = 0.234$. Shown are isotherms calculated with the help of DPIMC method. Temperature is given in units of thousand Kelvin.

model [2, 7] equations of state for hydrogen and helium are presented in tabular form [2]. Thermodynamic properties of hydrogen-helium mixtures can then be calculated by interpolation in composition between the two pure EOS. Using the so-called "linear mixing" it is possible approximately to calculate the density $\rho(P,T)$ of the hydrogen-helium mixture with the mass fraction of helium Y at pressure P and temperature T:

$$\frac{1}{\rho(P,T)} = \frac{1-Y}{\rho^{\mathrm{H}}(P,T)} + \frac{Y}{\rho^{\mathrm{He}}(P,T)}.$$

The results of comparison are shown in Fig. 1. The agreement between our calculations and the model [2] along the isotherms $T = 3\cdot 10^4$, $4\cdot 10^4$, $5\cdot 10^4$, and 10^5 K is quite

good and becomes better with the increase of temperature. The smaller values of pressure on the DPIMC isotherm $3 \cdot 10^4$ K near the particle density value 10^{23} cm^{-3} can be explained by a strong influence of bound states in this region; these effects are taken into account only approximately in the model [2]. The formation of atoms and molecules is also the reason of the pressure reduction along the 10^5 K isotherm with respect to the isotherm of non-interacting hydrogen-helium mixture.

In Fig. 2 the dependency of pressure vs. electron particle density along isotherms is shown. At high temperatures the isotherms have no peculiarities. However along the isotherm $T = 2 \cdot 10^4$ K there is a region for $n_e > 3 \cdot 10^{23}$ cm^{-3}, where our simulations do not reach the equilibrium state, the pressure strongly fluctuates and even becomes negative. Also along the isotherms $T = 10^4$ K and $T = 1.5 \cdot 10^4$ K there are two such regions 10^{22} cm$^{-3} < n_e < 10^{23}$ cm^{-3} and $n_e > 3 \cdot 10^{23}$ cm^{-3}. Earlier we found a similar effect for pure hydrogen at $T = 10^4$ K in the region of pressure ionization and showed that in the transition region a number of large clusters (droplets) were formed [25, 26]. Such behavior is typical for Monte Carlo simulations of metastable systems. In this region of pressure ionization the PPT was predicted by many authors [6, 7, 9–11, 27–29] and moreover a sharp electrical conductivity rise was measured in [30]. These instabilities in our calculations indicate the existence of PPT in dense hydrogen. Later [13] we found the PPT and the formation of droplets in electron-hole plasma of germanium semiconductor at low temperature and found good agreement with experimental data [31]. The appearance of clusters (droplets) in plasma leads to a drop of total energy of the system and Fig. 2 illustrates this fact. On isotherms one can see minima corresponding to the region where recombination of hydrogen molecules occurs. Under these conditions we observed the formation of molecules from the pair distribution functions analysis. The number of hydrogen molecules increases with the temperature drop. At low temperatures $T = 10^4$ and $2 \cdot 10^4$ K we observe the formation of large clusters of atoms and molecules.

The problem of PPT in a hydrogen-helium mixture is significantly determined by the composition of the mixture [2, 7, 29]. From shock-wave experiments one can estimate the range of temperature and density where a sharp electrical conductivity rise takes place. In quasi-isentropic compression the transition from a low-conductivity state to a high-conductivity one for hydrogen occurs at $T \sim 3-15$ kK and $\rho = 0.4-0.7$ g/cm^3 [30, 32] whereas for helium at $T = 15-40$ kK and $\rho = 0.7-1.25$ g/cm^3 [33]. However it is not enough to determine the region of existence of the PPT. According to theoretical equations of state for hydrogen and helium based upon the quantum statistical approach the critical point of the PPT in pure hydrogen is $T_{cr_H}^{(1)} = 14.9$ kK, $P_{cr_H}^{(1)} = 0.723$ Mbar in Ref. [29] and $T_{cr_H}^{(2)} = 15.3$ kK and $T_{cr_H}^{(2)} = 0.61$ Mbar in Refs. [2, 7]. In pure helium the critical point was found to be $T_{cr_{He}}^{(1)}$ = 17 kK, $P_{cr_{He}}^{(1)}$ = 7.22 Mbar [29]. At helium mass concentration $Y < 0.93$ and temperature less than both critical temperatures the properties of hydrogen-helium mixture are determined mostly by hydrogen and only one PPT exists. At high values of $Y > 0.93$ both the hydrogen and helium PPT can occur for the same temperature. In our DPIMC simulations we have observed one PPT at $T = 2 \cdot 10^4$ K and two PPTs at $T = 10^4$ K even at $Y = 0.234$. The results of our simulation are shown in Fig. 3 together with experimental data and theoretical predictions.

Along the isotherm $T = 2 \cdot 10^4$ K we found the region with bad convergence in the

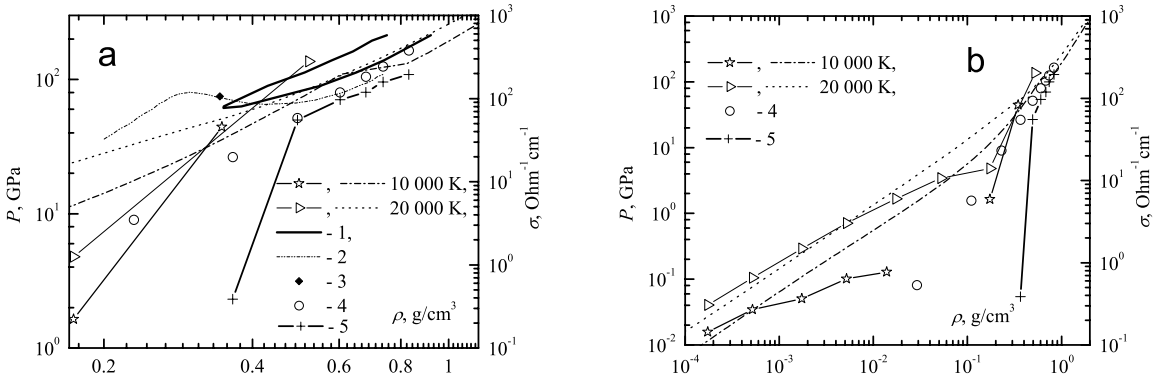

FIGURE 3. The DPIMC (lines with asterisks and triangles) and theoretical (dashed and dash - dotted lines) [2, 7] isotherms for pressure in a hydrogen-helium mixture with the mass concentration of helium $Y = 0.234$ vs. density. 1 — phase boundaries of PPT in hydrogen [2, 7], 2 — undercritical metastable isotherm $T = 1.2 \cdot 10^4$ K and $Y = 0.308$ [29], 3 — critical point of PPT in hydrogen-helium mixture with $Y = 0.308$ [29]. Also shown are experimental results of Ref. [34]: 4 — quasi-isentrope of hydrogen-helium mixture, $T \sim 5000$ K, 5 — electrical conductivity of hydrogen along the quasi-isentrope (right axis). Left picture is the enlargement of the high density part of the right figure.

range of densities between 0.5 and 5 g/cm^3. Along the isotherm $T = 1.5 \cdot 10^4$ K and $T = 10^4$ K such region is even wider and begins from 0.38 g/cm^3. Surprisingly there was another region where pressure became negative: from 0.015 to 0.19 g/cm^3. The nature of this phenomenon is currently unclear for us. From Fig. 3 it can be easily seen that other predictions of PPT in hydrogen or hydrogen-helium mixtures [2, 29] with low mass concentration of helium are located in the beginning of the region where DPIMC simulation fails to converge to the equilibrium state. The sharp rise of electrical conductivity of hydrogen-helium mixture along the quasi-isentrope with the initial state $T = 77.4$ K and $P = 8.1 \cdot 10^-3$ GPa is also observed experimentally in the range of densities 0.5–0.83 g/cm^3 [34], see line with crosses in Fig. 3a.

ACKNOWLEDGMENTS

This work is done under financial support of RF President Grant No. MK-1769.2003.08, the RAS program No. 17 "Parallel calculations and multiprocessor computational systems", the grant for talented young researchers of the Science support foundation and the Deutsche Forshungsgemeinschaft under grant BO 1366-2. The research was also partly sponsored by Award No. PZ-013-02 of the U.S. Civilian Research & Development Foundation for the Independent States of the Former Soviet Union (CRDF) and of Ministry of Education of Russian Federation. The calculations were perfomed thanks to a grant for CPU time at the NIC Jülich.

REFERENCES

1. Chabrier, G., Saumon, D., Hubbard, W. B., and Lunine, J. I., *Astrophys. J.*, **391**, 817–826 (1992).
2. Saumon, D., Chabrier, G., and Van Horn, H. M., *Astrophys. J. Suppl. Ser.*, **99**, 713–741 (1995).
3. Gudkova, T. V., and Zharkov, V. N., *Planet. Space Sci.*, **47**, 671–677 (2000).
4. Nellis, W. J., *Planet. Space Sci.*, **48**, 671–677 (2000).
5. Beule, D., Ebeling, W., Förster, A., Juranek, H., Redmer, R. and Röpke, G., *Journal de Physique IV, (Proceedings)*, **10, Pr5**, 295–299 (2000).
6. Saumon, D., and Chabrier, G., *Phys. Rev. A*, **44**, 5122–5141 (1991).
7. Saumon, D., and Chabrier, G., *Phys. Rev. A*, **46**, 2084–2100 (1992).
8. Fortov, V. E., Ternovoi, V. Y., Zhernokletov, M. V., Mochalov, M. A., Mikhailov, A. L., Filimonov, A. S., Pyalling, A. A., Mintsev, V. B., Gryaznov, V. K., and Iosilevskii, *JETP*, **97**, 259–278 (2003).
9. Norman, G. E., and Starostin, A. N., *Sov. Phys. High Temp.*, **6**, 410 (1968).
10. Ebeling, W., Kraeft, W. D., and Kremp, D., *Theory of Bound States and Ionization Equilibrium in Plasmas and Solids*, Akademie-Verlag, Berlin, 1976.
11. Kraeft, W. D., Kremp, D., Ebeling, W., and Röpke, G., *Quantum Statistics of Charged Particle Systems*, Akademie, Berlin, 1986.
12. Zamalin, V. M., Norman, G. E., and Filinov, V. S., *The Monte-Carlo Method in Statistical Thermodynamics*, Nauka, Moscow, 1977.
13. Filinov, V. S., Bonitz, M., Levashov, P. R., Fortov, V. E., Ebeling, W., Schlanges, M., and Koch, S. W., *J. Phys. A.: Math. Gen.*, **36**, 6069–6076 (2003).
14. Feynman, R. P., *Statistical Mechanics*, Advanced Book Program, Reading, Massachusetts, 1972.
15. Kalman, G., editor, *Strongly Coupled Coulomb Systems*, Pergamon, Oxford, 1988.
16. Ebeling, W., Hoffmann, H. J., and Kelbg, G., *Contrib. Plasma Phys.*, **7**, 233 (1967).
17. Filinov, A. V., Bonitz, M., and Ebeling, W., *J. Phys. A: Math. Gen.*, **36**, 5957–5962 (2003).
18. Filinov, V. S., Bonitz, M., and Ebeling, W., and Fortov, V. E. *Plasma Phys. Contr. Fusion*, **43**, 743 (2001).
19. Filinov, V. S., Levashov, P. R., Fortov, V. E., and Bonitz, M., "Thermodynamic properties of correlated strongly degenerate plasmas," in *Progress in Nonequilibrium Green's Functions*, edited by M. Bonitz, World Scientific, Singapore, 2000, pp. 513–520.
20. Filinov, V. S., Bonitz, M., and Fortov, V. E., *JETP Letters*, **72**, 245–248 (2000).
21. Filinov, V. S., Fortov, V. E., Bonitz, M., and Kremp, D., *Phys. Lett. A*, **274**, 228–235 (2000).
22. Bezkrovniy, V., Filinov, V. S., Kremp, D., Bonitz, M., Schlanges, M., Kraeft, W. D., Levashov, P. R., and Fortov, V. E., *Phys. Rev. E* (accepted, 2004).
23. Knudson, M. D., Hanson, D. L., Bailey, J. E., Hall, C. A., and Assay, J. R., *Phys. Rev. Lett.*, **90**, 035505–1 (2003).
24. Da Silva, L. P., Celliers, P., et al., *Phys. Rev. Lett.*, **78**, 483–486 (1997).
25. Filinov, V. S., Fortov, V. E., Bonitz, M., and Levashov, P. R., *JETP Letters*, **74**, 384 (2001).
26. Levashov, P. R., Filinov, V. S., Fortov, V. E., and Bonitz, M., "Thermodynamic Properties of Nonideal Strongly Degenerate Hydrogen Plasma," in *Shock Compression of Condensed Matter — 2001*, edited by M. D. Furnish, N. N. Thardhani, and Y. Horie, AIP, New York, 2002, pp. 119–126.
27. Saumon, D., and Chabrier, G., *Phys. Rev. Lett.*, **62**, 2397 (1989).
28. Yan, X., Tsai, S., and Ichimaru, S., *Phys. Rev. A*, **43**, 3057 (1991).
29. Schlanges, M., Bonitz, M., and Tschttschjan, A., *Contrib. Plasma Phys.*, **35**, 109–125 (1995).
30. Ternovoi, V. Y., Filimonov, A. S., Fortov, V. E., Kvitov, S. V., Nikolaev, D. N., and Pyalling, A. A., *Physica B*, **265**, 6–11 (1999).
31. Thomas, G. A., Rice, T.-M., and Hensel, J. C., *Phys. Rev. Lett.*, **33**, 219–222 (1974).
32. Weir, S. T., Mitchell, A. C., and Nellis, W. J., *Phys. Rev. Lett.*, **76**, 1860–1863 (1996).
33. Ternovoi, V. Y., Filimonov, A. S., Pyalling, A. A., Mintsev, V. B., and Fortov, V. E., "Thermophysical properties of helium under multiple shock compression," in *Shock Compression of Condensed Matter — 2001*, edited by M. D. Furnish, N. N. Thardhani, and Y. Horie, AIP, New York, 2002, pp. 107–110.
34. Ternovoi, V. Y., Kvitov, S. V., Pyalling, A. A., Filimonov, A. S., and Fortov, V. E., *JETP Letters*, **79**, 8–11 (2004).